Metallomics

Accepted Manuscript

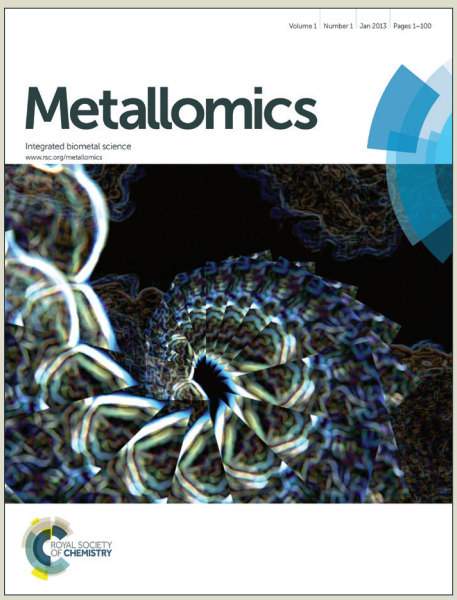

This is an *Accepted Manuscript*, which has been through the Royal Society of Chemistry peer review process and has been accepted for publication.

Accepted Manuscripts are published online shortly after acceptance, before technical editing, formatting and proof reading. Using this free service, authors can make their results available to the community, in citable form, before we publish the edited article. We will replace this *Accepted Manuscript* with the edited and formatted *Advance Article* as soon as it is available.

You can find more information about *Accepted Manuscripts* in the Information for Authors.

Please note that technical editing may introduce minor changes to the text and/or graphics, which may alter content. The journal's standard Terms & Conditions and the Ethical guidelines still apply. In no event shall the Royal Society of Chemistry be held responsible for any errors or omissions in this *Accepted Manuscript* or any consequences arising from the use of any information it contains.

ROYAL SOCIETY OF CHEMISTRY

www.rsc.org/metallomics

Table of content entry:

Through electronic and structural models, the factors influencing coordination sphere expansion of structural zinc in proteins are discussed

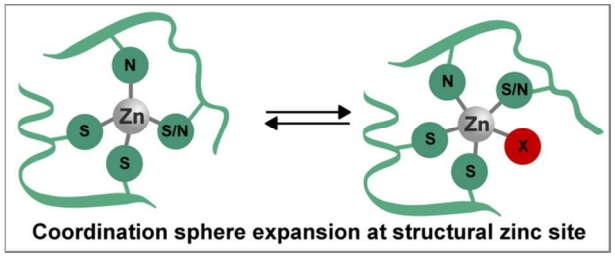

Coordination sphere expansion at structural zinc site

Metallomics Accepted Manuscript

Cite this: DOI: 10.1039/c0xx00000x

www.rsc.org/xxxxxx

ARTICLE TYPE

The Dynamics of Zinc Sites in Proteins: Electronic Basis for Coordination Sphere Expansion at Structural Sites

A. Gerard Daniel[a] and Nicholas P. Farrell*[a]

Received (in XXX, XXX) Xth XXXXXXXXX 20XX, Accepted Xth XXXXXXXXX 20XX

DOI: 10.1039/b000000x

The functional role assumed by zinc in proteins is closely tied to the variable dynamics around its coordination sphere arising by virtue of its flexibility in bonding. Modern experimental and computational methods allow the detection and study of previously unknown features of bonding between zinc and its ligands in protein environment. These discoveries are occurring just in time as novel biological functions of zinc, which involve rather unconventional coordination trends, are emerging. In this sense coordination sphere expansion of structural zinc sites, as observed in our previous experiments, is a novel phenomenon. Here we explore the electronic and structural requirements by simulating this phenomenon in structural zinc sites using DFT computations. For this purpose, we have chosen MPW1PW91 and a mixed basis set combination as the DFT method through benchmarking, because it accurately reproduces structural parameters of experimentally characterized zinc compounds. Using appropriate models, we show that the greater ionic character of zinc coordination would allow for coordination sphere expansion if the steric and electrostatic repulsions of the ligands are attenuated properly. Importantly, through the study of electronic and structural aspects of the models used, we arrive at a comprehensive bonding model, explaining the factors that influence coordination of zinc in proteins. The proposed model along with the existing knowledge would enhance our ability to predict zinc binding sites in proteins, which is today of growing importance given the predicted enormity of the zinc proteome.

Introduction

The electronic properties of Zn^{2+}, such as intermediate Lewis acidity, redox inertness and flexible coordination geometry, render it a suitable cofactor in several proteins that perform essential biological functions. The role of Zn^{2+} in these proteins is broadly classified as catalytic, structural and regulatory. Zinc in proteins is usually tetracoordinate adopting a distorted tetrahedral geometry.[1] However, the number and type of protein ligands that are bound to zinc dictates the dynamics and hence the functionality of a given site (Fig. 1). For example, in catalytic sites, Zn^{2+} is bound to three protein ligands with histidine being the most commonly occurring ligand. The fourth coordination position, which is often occupied by a water molecule, can be considered open because it is dynamic and undergoes fast exchange with the substrate, as required for catalysis.[2,3] In addition to these classical catalytic zinc sites, sites where zinc expands its coordination sphere temporarily to a pentacoordinate state to accommodate the substrate are also known.[3] This includes the earliest characterized zinc enzyme, carbonic anhydrase II. On the other hand, structural zinc sites are characteristic of Zn^{2+} bound to all four protein ligands, which are almost exclusively comprised of cysteine and histidine, with a greater occurrence of cysteine. These sites possess a high binding affinity towards Zn^{2+}.

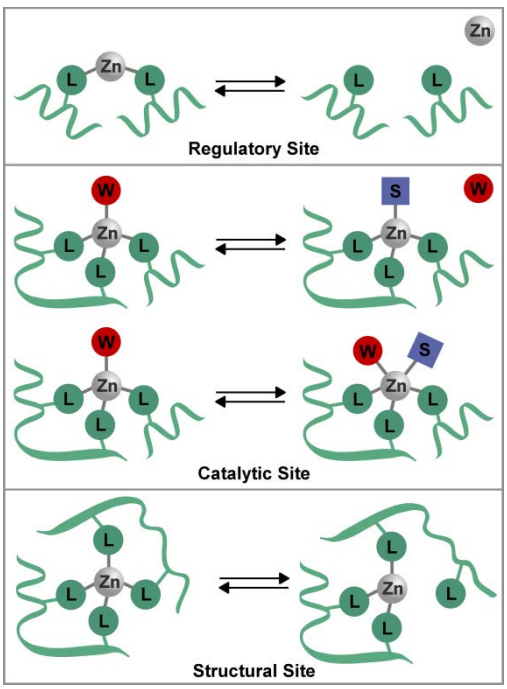

Fig. 1 Variable dynamics at different types of zinc sites in proteins as a function of the number of protein ligands bound to Zn^{2+}. L represents amino acid ligands; W stands for H_2O or OH^-; S is substrate or inhibitor.

Metallomics Accepted Manuscript

Thus, they were considered more stable and static, until recently.[1] Several studies have now shown that the sulphur-rich structural sites are reactive and dynamic due to their intrinsic instability (discussed below).[4-7] Further, instances of zinc bound to just two protein ligands are known in regulatory sites.[8]

Dynamics of Regulatory Zinc Sites

Following the findings that several cellular enzymes are inhibited by Zn^{2+}, the role of Zn^{2+} as a regulator of cellular processes is the focus of much current research. An interesting aspect of this new role of Zn^{2+} is the unique coordination chemistry at these sites, although structural data of inhibitory Zn^{2+} sites are sparse at this time. However, from the available information, it can be inferred that these sites feature fewer and uncommon protein ligands.[8] Zinc at regulatory sites is often bound to just two protein ligands. Hence, these sites possess low metal binding affinity, allowing reversible binding of Zn^{2+} to the protein and enabling control over its function.

Zinc and Caspases

Among the enzymes that may be regulated by zinc are caspases, the apoptotic proteases, which are targets for drug development. In a recent report, we have deduced an inhibitory zinc site in caspase-3 using experimental and theoretical approaches.[9] The proposed site, constituted of the catalytic histidine (His121) and a nearby methionine (Met61), consistently fits the experimental observations better than does the generally assumed inhibitory site, the catalytic dyad (His121 & Cys163). Further the newly proposed site is 11 kcal mol^{-1} more stable than zinc binding to the catalytic dyad. The preference of methionine, which is not a common zinc ligand, over cysteine at this site, serves as an example of how the general conventions in Zn^{2+} coordination can be effectively overridden through factors dictated by the protein environment.

Dynamics of Structural Zinc Sites

Zinc finger (ZF) proteins, which are the most commonly occurring structural zinc sites, are classified based on the number of cysteine and histidine ligands in the primary coordination sphere of Zn^{2+}; these are Cys_2His_2, Cys_3His and Cys_4 type cores.[10] For a while now, it is known that Zn-Cys_4 moiety is employed in nucleophilic reactions, with one of the sulphurs undergoing S-alkylation reaction.[4,5] Coordination to zinc helps deprotonation of the cysteine leading to increased nucleophilicity of the sulphur. Further, given the stability of the "full" coordination spheres, inferred through measurement of K_ds from picomolar to femtomolar range,[11,12] structural zinc sites were considered to be static and unreactive. However, recently, several experimental and theoretical studies have identified structural zinc sites as dynamic and labile.[6,7,13-16] These findings are crucial to understand zinc exchange and transport in biology[17,18] and the reactivity of structural zinc sites towards drugs, such as electrophiles and metal chelators. Due to this intrinsic reactivity, zinc finger proteins have become popular drug targets, especially in cancer and retroviral therapy.[19-21] In this context, we have developed metal-centred electrophiles for targeting ZF cores.[22-24] These electrophiles target the nucleophilic thiolates of the ZFs to form adducts eventually leading to ejection of zinc and loss of protein function.

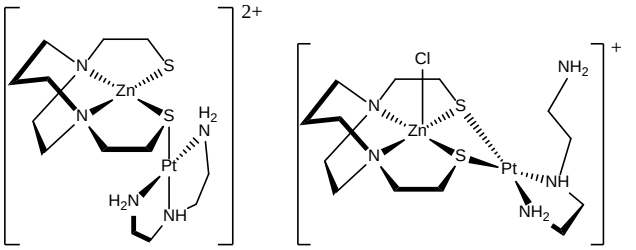

Fig. 2. Structures of complexes formed during a reaction of $[PtCl(dien)]^+$ and $[Zn(bme\text{-}dach)]_2$.[25]

Coordination Sphere Expansion in Structural Sites

An uncommon trend in coordination of Zn^{2+} was observed in previous studies from our laboratory involving structural zinc sites and Pt electrophiles. The product of the interaction of $[PtCl(dien)]^+$ (dien = diethylenetriamine) with a zinc finger model compound, $[Zn(bme\text{-}dach)]_2$, is initially $[Zn(bme\text{-}dach)(Pt(dien))]^{2+}$ (**I**) the product of electrophilic attack of a [Pt(dien)] moiety on the chelate with formation of a monothiolate Zn-SR-Pt bridge (Fig. 2).[25] A second species with a mass to charge ratio corresponding to $[(Zn(bme\text{-}dach)Cl)(Pt(dien))]^+$, **II**, is also observed.[25] Isolation of the latter species and characterization by X-ray crystallography showed Pt^{2+} bound through a dithiolate bridge to Zn^{2+} and Cl^- bound to the zinc ion, Fig. 2. These results were mirrored in the reaction of $[PtCl(dien)]^+$ with the C-terminal zinc finger of the HIV nucleocapsid NCp7 protein (ZFI), where mass spectrometry showed the formation of ZFI:[Pt(dien)] adducts by thiolate displacement of Cl in the Pt-Cl bond, accompanied by a companion peak corresponding to a 1:1 adduct of ZFI:$[PtCl(dien)]^+$.[22] By analogy with the model compound study zinc pentacoordination was hypothesized, with monofunctional Pt bound to the ZFI through a bridging thiolate while Cl^- acts as the fifth ligand to Zn^{2+}. From PDB surveys it is clear that the common protein ligands in pentacoordinate catalytic zinc sites are either N or O donors and it is a rarity to find cysteine as a ligand at pentacoordinate sites.[1] Thus the results represent unique cases where pentacoordination is suggested in the presence of multiple cysteine ligands.

The Hidden Dynamics of Zinc sites

Several years after the discovery of the crucial involvement of zinc in biology, its properties still present surprises. The element itself is anomalous in several ways compared to its congeners, making it harder for strict classifications.[26] Hence, there exists a lack of consensus about important aspects such as nature of bonding and coordination flexibility of zinc (discussed below). The incompatibility of many common spectroscopic techniques that would otherwise help to study zinc proteins at the molecular level has been detrimental. However, site directed mutagenesis and metal substitution in conjunction with conventional biophysical techniques and X-ray crystallography have greatly helped towards the current understanding of zinc biochemistry.[27,28] X-ray crystal structure being the only data to obtain accurate structural information about zinc sites, much of the structural dynamics remains to be discovered. The increasing awareness of the dynamic role of zinc in cellular processes demands a better understanding of the mechanism involved in

Metallomics Accepted Manuscript

zinc transport, homeostasis and siganlling.[8,17,18,29-31] Recent improvements in experimental and theoretical methods, however, have allowed us to uncover some of these mysteries.[32]

Modern techniques for detection and characterization of zinc metalloproteins such as X-ray absorption spectroscopy (XAS), X-ray absorption fine structure spectroscopy (XAFS), nuclear magnetic resonance spectroscopy (NMR), electrospray ionization mass spectrometry (ESI-MS) and molecular dynamics (MD) offer an opportunity to explore the dynamics of Zn molecular systems. These methods need to be augmented by theoretical simulations for parameter fitting or by computational methods such as semi-empirical or density functional theory (DFT) methods for producing the structural details around zinc.[33-35] Quantum mechanical (QM) methods have become an indispensible tool for structure prediction of metal centres in proteins. Especially, the potential of QM methods to predict transition state and reaction intermediates is unprecedented. Particularly, among the QM methods, DFT is popular because it produces accurate results comparable to wave function-based post Hartree-Fock methods, yet in a cost effective manner.[36]

Various biologically relevant zinc cores have been modelled using DFT methods in order to study their basic properties. Important questions addressed by these studies are bonding and structural preferences,[37-39] nucleophilicity of zinc bound Cys and the effect of electrostatic screening from stabilizing groups,[40-43] the protonation state of zinc bound Cys and His[44-46] and the thermodynamic stability of the cores.[39,47] It has been proposed that solvent accessibility of the core and the higher charge accepting ability of zinc are the factors that favour tetracoordination.[48] It was also shown that, although sulphur-rich cores are thermodynamically stable, the Zn-L bonds are kinetically labile due to charge repulsion between the comparatively larger thiolate ligands.[7,47] Further, owing to the diffuseness of charge on the thiolates and the resulting coulomb repulsion, it has been inferred that the negatively charged Cys_4 or Cys_3His ZF cores would not permit the addition of another ligand.[37,47] However, since covalent attachment of Pt to the thiolates, as described above[22,25], would reduce the charge density on the sulphur atoms the coordination expansion that is observed in our experiments could be possible. Further, these kinetically unstable cores are known to be stabilized in proteins by hydrogen bonding interactions from the backbone N-H or from basic amino acids such as Lys and Arg.[49] These observations lead to the important question of whether such interactions could allow dynamic coordination sphere expansion of structural zinc sites resulting in transient species which may or may not serve a biological function. Since transient coordination sphere expansion is implicated in the catalytic mechanism of many zinc metalloenzymes, an understanding of the factors involved in such expansion is fundamental for a full description of the role of zinc biology. Here, we report DFT modelling of Cys_2His_2 and Cys_3His ZF cores, which we have used in our previous experimental studies, to understand the nature of bonding and stabilizing interactions that may lead to structural dynamics in the form of coordination sphere expansion at these sites.

Methods

Choice of DFT Method

During our preliminary studies, we found that popular density functionals, such as B3LYP[50,51] and SVWN[52,53] that are often used for geometry optimization of zinc molecular models, were not suited for our purpose (discussed later). Hence we opted to benchmark a few select DFT methods against a known experimental structure (Fig. 2 **II**) that closely resembles the models of our interest. The details of the benchmarking process and the validation of the chosen method can be found in the supporting information. Through the process, we chose to use MPW1PW91 functional and a mixed basis set, mBS5, which constitutes, 6-311G basis set for C, N, S and Cl atoms with 3df polarization functions on N and S atoms; d polarization function on C and Cl; p polarization on H; diffuse functions on S and Cl, which are anionic ligating atoms; the Wachters-Hay all electron basis set[54,55] for Zn with 3fg polarization functions and Lanl2DZ basis set with effective core potential for Pt in all calculations involving Pt. The computations are performed using Gaussian03 suite of programs.[56] The structure of complexes were optimized at MPW1PW91/mBS5 level. Frequency calculations were performed in all cases to confirm that the optimized geometry is a minimum on the potential energy surface. The electronic energy (E) of complexes reported here includes thermal and zero-point energy corrections.

Modelling of Structural Zinc Sites

For computational efficiency and simplicity, usually histidine ligands are modelled as imidazole and cysteine as thiomethane (Fig. 3). However, such minimal models do not account for the stabilization arising from interaction between the backbone amide N–H and S of zinc bound thiolate. These interactions are known to attenuate the electrophilicity of the participating thiolate and may help in stabilizing the pentacoordination state, under study. Therefore, we included an amide bond in the thiolate ligands by extending the thiomethane ligands to 3-sulfanylpropanamide. The resulting optimal models would mimic the protein environment better than continuum solvent models. In cases where there is no need for such interaction, as will be mentioned, the thiolates were simply modelled as thiomethane. In some of the models, stabilizing interactions from Lys were modelled using ammonium ions.

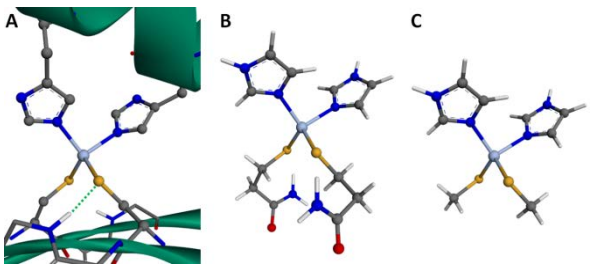

Fig. 3 Possible levels of reduction for modelling structural zinc sites: (A) a C_2H_2 type zinc finger site: stabilizing N–H···S are present (B) optimal model where histidine is modelled as imidazole and cysteine modelled using 3-sulfanylpropanamide (C) minimal model where the backbone stabilization is neglected.

Metallomics Accepted Manuscript

Cite this: DOI: 10.1039/c0xx00000x

www.rsc.org/xxxxxx

ARTICLE TYPE

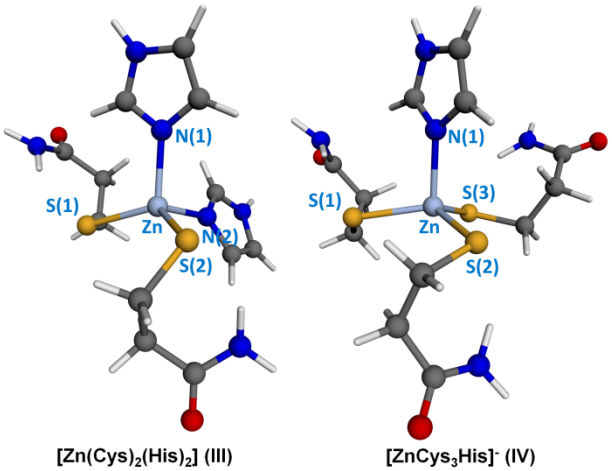

[Zn(Cys)$_2$(His)$_2$] (III) [ZnCys$_3$His]$^-$ (IV)

Complex III			
Bond lengths (Å)		NBO charges (e)	
Zn-N(1)	2.087	Zn	1.55
Zn-N(2)	2.086	N(1)	-0.68
Zn-S(1)	2.263	N(2)	-0.69
Zn-S(2)	2.278	S(1)	-0.66
		S(2)	-0.64

Complex IV			
Bond lengths (Å)		NBO charges (e)	
Zn-N(1)	2.142	Zn	1.51
Zn-S(1)	2.310	N(1)	-0.64
Zn-S(2)	2.315	S(1)	-0.68
Zn-S(3)	2.312	S(2)	-0.66
		S(3)	-0.69

Fig. 4. Optimized structures of Cys$_2$His$_2$ and Cys$_3$His ZF models: the M-L bond distances and NBO charges on the metal and the ligating atoms are listed.

Results and Discussion

ZF model systems

Geometry of Cys$_2$His$_2$ and Cys$_3$His ZF cores

Having chosen an appropriate DFT method for modelling structural zinc sites, we optimized the geometries of [Zn(Cys)$_2$(His)$_2$] (**III**) and [Zn(Cys)$_3$(His)]$^-$ (**IV**) models (Fig. 4). The optimized structures resulted in distorted tetrahedral geometries for both the models. The metal-ligand (M-L) bond lengths, tabulated in Fig. 4, are very comparable to the average values obtained from X-ray crystal structure data of zinc complexes,[44] which once again validates the DFT method used. To our knowledge this is the first time such accuracies in bonding parameters have been reached for modelling ZF cores using DFT in gas phase. For [Zn(Cys)$_2$(His)$_2$], the ∠S-Zn-S measures 121.0°, the average ∠S-Zn-N is 108.5 ± 2.5° and ∠N-Zn-N is 99.4°. In the case of [Zn(Cys)$_3$(His)]$^-$, the average ∠S-Zn-S is 115.5 ± 3.1°, the average ∠S-Zn-N is 102.4 ± 3.9°. The distortion in the structures, apparent from these angles, is partly due to coulomb repulsion between ligands, as proposed by an early study.[57] The soft or diffuse anionic thiolate ligands tend to stay as far away as possible, while, the smaller neutral imidazoles are forced to near perpendicular conformation with respect to each other while the ∠S-Zn-N stays midway. In [Zn(Cys)$_3$(His)]$^-$, the three thiolates are in a near planar conformation with the imidazole perpendicular to them. Here, the ∠S(1)-Zn-N and ∠S(2)-Zn-N are around 100° but the ∠S-Zn-N is 106°. This variation is presumably due to stabilizing interaction between the hydrogens of imidazole ring with S(1) and S(2) which is absent for S(3). The larger ∠S-Zn-S in this complex is due to van der Waals interaction between the C_β-H of one of the thiolate ligands to the S of the neighbouring ligand. Further, as previously observed,[44] an elongation of Zn-L bonds is observed in [Zn(Cys)$_3$(His)]$^-$ possibly due to the increased repulsive force arising from the excess charge on the complex. Further, in both the complexes stabilization of zinc bound thiolates by the amide N–H can be seen from the orientation of N-H bond towards the thiolate lone pair, with an average S···H distance of 2.27 ± 0.04 Å. Thus stabilizing secondary sphere interactions and repulsive interactions should be accounted in order to properly explain the structure and possibly the dynamics at these sites.

The Electronic structure and bonding of ZF cores

As can be seen from the natural bond orbital (NBO) analysis, all the ligating atoms have almost similar charge. However, the charge resides on a more diffuse 3p orbital for S compared to the compact 2p orbital for N, which accounts for the large repulsive force produced by the thiolate ligands. The charge transferred from the ligands to zinc, which correlates to the degree of covalency, is 0.5 e for both these complexes. Previous theoretical studies have shown that the M-L bond in zinc complexes are 80% ionic and 20% covalent in character, which is in agreement with this result.[47] Comparing the two ZF cores there is no big difference in the charge transfer to Zn. Along with the fact that elongation of Zn-L bond lengths would reduce the overlap and hence the charge transfer, it can be said that the observed small variation of charge on Zn is due to change in overall charge of the system rather than due to preferential charge acceptance from S ligands.[37] Further, from natural population analysis (NPA, Table S1) it is found that almost all of the charge accepted by Zn resides in its 4s orbital. Thus, the predominant ionic character along with the spherical nature of the 4s orbital, which is involved in the most favourable covalent interaction, allows zinc to adapt a flexible coordination sphere unlike the other transition metals where metal d orbitals participate in bonding, dictating the geometry. Although zinc would not enforce any directionality, in order to maximize electrostatic attractions, the ligand p orbitals need to be oriented properly. Given the large ionic contribution to

Metallomics Accepted Manuscript

bonding, the best model to describe bonding in biological tetracoordinate zinc complexes is given by Picot *et al*.[47] In this model, the electronic structure of the complexes is represented by four resonance structures each showing one bond pair, between Zn and one of the ligands, and three ionic bonds between Zn and the other ligands.

Interaction of $[Pt(dien)]^{2+}$ with ZF cores

Next, we determined the effect of covalent binding of a Pt electrophile, $[Pt(dien)]^{2+}$, on the thiolates of ZF cores under investigation. For this purpose, we optimized the structures of monothiolate and dithiolate bridged Zn-Pt binuclear complexes where zinc is still tetracoordinate. In the dithiolate bridged complexes the second S was bound to Pt in place of a terminal amino group of the dien ligand. The structures, M-L bond lengths and NBO charges on the metals and ligating atoms are shown in

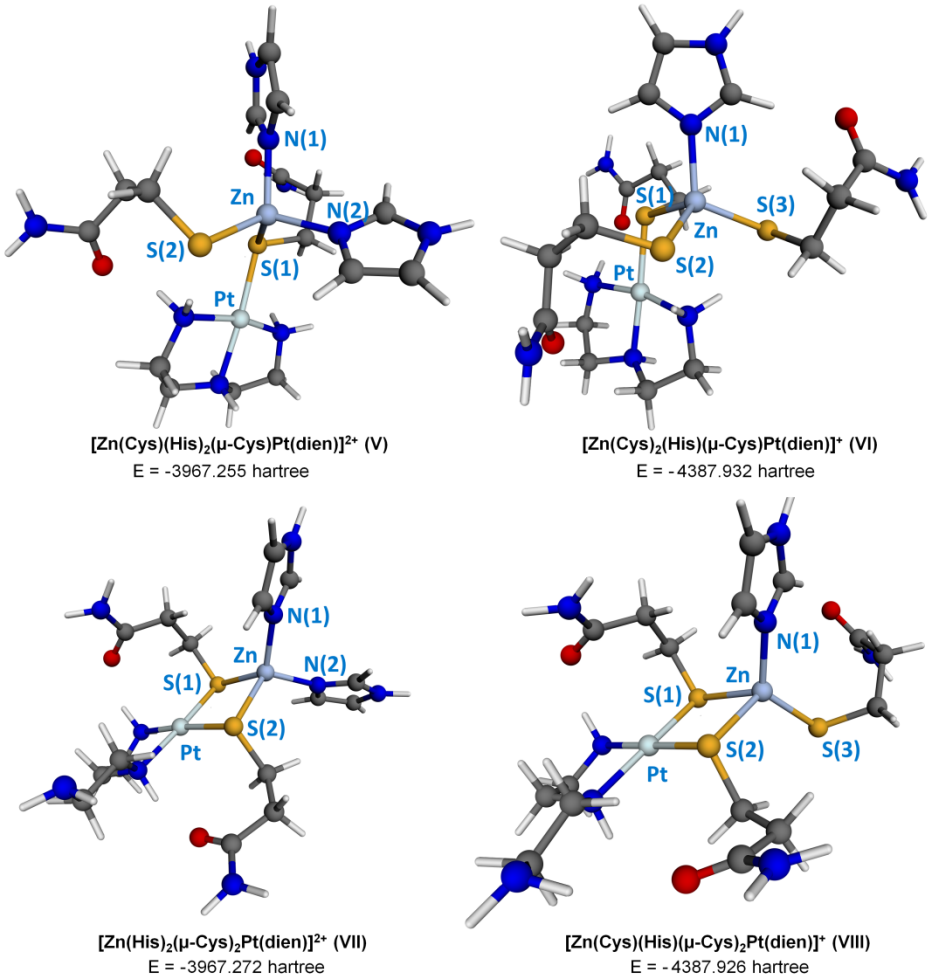

Complex V			
Bond lengths (Å)		NBO charges (e)	
Zn-N(1)	2.019	Zn	1.59
Zn-N(2)	2.037	N(1)	-0.75
Zn-S(1)	2.423	N(2)	-0.72
Zn-S(2)	2.267	S(1)	-0.36
Pt-S(1)	2.317	S(2)	-0.64
		Pt	0.63

Complex VI			
Bond lengths (Å)		NBO charges (e)	
Zn-N(1)	2.034	Zn	1.52
Zn-S(1)	2.443	N(1)	-0.71
Zn-S(2)	2.294	S(1)	-0.40
Zn-S(3)	2.296	S(2)	-0.65
Pt-S(1)	2.318	S(3)	-0.66
		Pt	0.63

Complex VII			
Bond lengths (Å)		NBO charges (e)	
Zn-N(1)	2.009	Zn	1.59
Zn-N(2)	2.014	N(1)	-0.74
Zn-S(1)	2.341	N(2)	-0.74
Zn-S(2)	2.353	S(1)	-0.37
Pt-S(1)	2.320	S(2)	-0.39
Pt-S(2)	2.343	Pt	0.48

Complex VIII			
Bond lengths (Å)		NBO charges (e)	
Zn-N(1)	2.022	Zn	1.51
Zn-S(1)	2.426	N(1)	-0.72
Zn-S(2)	2.423	S(1)	-0.31
Zn-S(3)	2.234	S(2)	-0.38
Pt-S(1)	2.298	S(3)	-0.62
Pt-S(2)	2.312	Pt	0.46

Fig. 5. Optimized structures of monothiolate and dithiolate bridged Zn-Pt binuclear tetracoordinate Zn complexes of Cys_2His_2 and Cys_3His ZF cores. The M-L bond distances and NBO charges on the metals and the ligating atoms are also listed.

Fig. 5. All of these structures were found to be minima with intact mono or dithiolate Pt-$(SR)_n$-Zn bridges. In all complexes the Pt centre is square planar, as expected, with ∠L-Pt-L angles around 90°. The small deviations observed in these angles are mostly due to steric interactions. In the monothiolate bridged Cys_2His_2 complex, **V** (Fig. 5), the ∠S-Zn-S measures 111.2°, the average ∠S-Zn-N is 110.5 ± 2.1° and ∠N-Zn-N is 103.5°. In the case of dithiolate bridged complex of the same core, **VII** (Fig. 5), the ∠S-Zn-S is 88.6°, the average ∠S-Zn-N is 115.4 ± 8.6° and ∠N-Zn-N is 106.5°. Similar trends were observed for the complexes of Cys_3His core. Here, for the monothiolate bridged, **VI** (Fig. 5), the average ∠S-Zn-S measures 108.6 ± 4.7°, the average ∠S-Zn-N is 109.8 ± 6.8°. And, for the dithiolate bridged **VIII** (Fig. 5), the ∠S(1)-Zn-S(2), involving both the bridging thiolates measures 83.4° and the average of other ∠S-Zn-S is 110.6 ± 4.8°, the average ∠S-Zn-N is 114.5 ± 13.5°. These values, when compared to the cores by themselves, reveal relaxation of ∠S-Zn-N and ∠N-Zn-N with a reduction in ∠S-Zn-S, which is obviously due to reduction of charge on the Pt bound S atom. The Zn-S bonds to the bridging thiolates are elongated but are well within the range observed in proteins,[34] while the Zn-S bonds of non-bridging thiolates shorten a little. A shortening of Zn-N bonds is also observed. All of these changes arise due to lower charge repulsion between the ligands as a result of stabilization from the Pt centre. In addition, the non-bridging thiolates could now be stabilized by the N-H group of the dien ligand. This is more effective than the stabilization arsing from amide N-H. This interaction is reminiscent of Lys-thiolate interaction in zinc finger

Metallomics Accepted Manuscript

proteins, which is common. The observed larger deviations in the bond angles of these systems are due to these stabilizing interactions or sometimes due to steric avoidance of the C-H groups.

There is a small increase in the positive charge on Zn for the Cys_2His_2 core. This once again may just reflect the increase in overall charge of the complex than the charge transfer capacity of the ligands. Compared to S of the non-bridging thiolates, there is an approximate 0.3 e transferred to Pt by the S on the bridging thiolates. By comparing the charge on Pt from the monothiolate and dithiolate bridged analogues, it is clear that the amount of charge transfer to Pt depends on the number of thiolate ligands. This indicates stronger covalent character of Pt-S bonds, which leads to a large reduction of charge on thiolates. The Pt-S bonds are of normal lengths as observed in crystal structures,[25] which indicates a strong bonding between Pt and S. From NPA it can be seen that most of the charge transferred is from the S 3p orbital. The reduction of 0.3 e from the S 3p orbitals helps reduce the

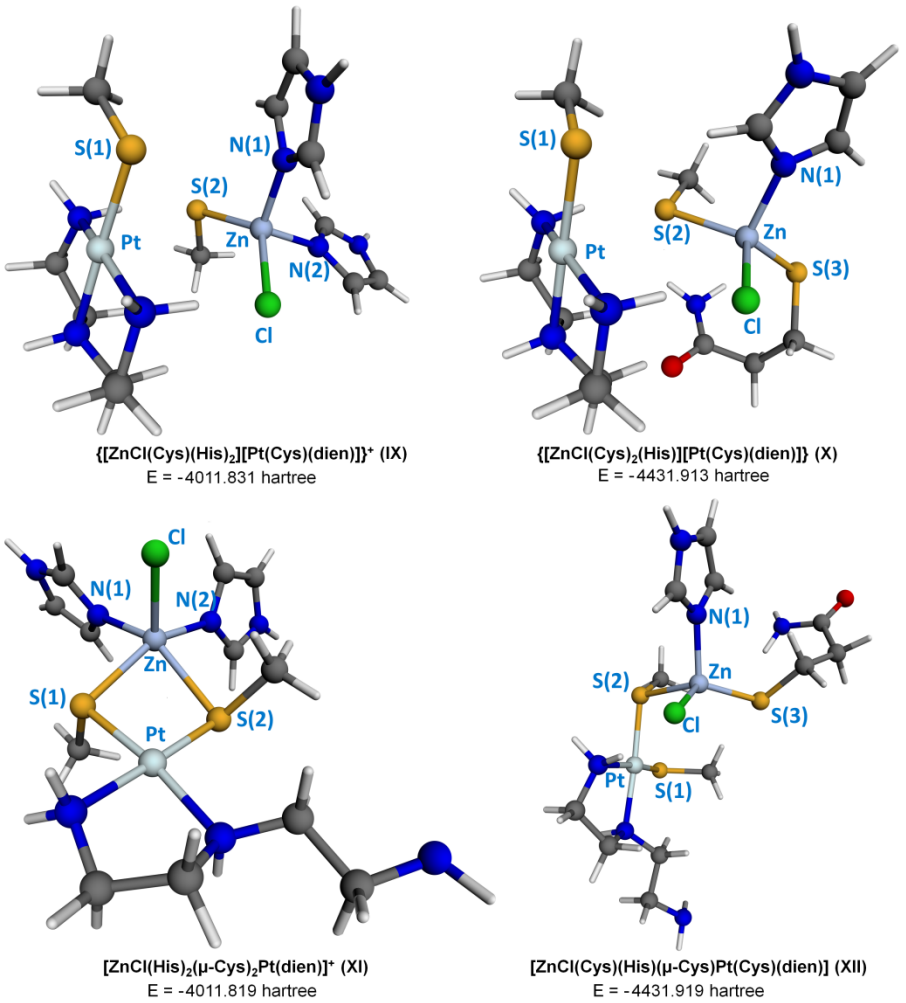

Complex IX			
Bond lengths (Å)		NBO charges (e)	
Zn-Cl	2.332	Zn	1.6
Zn-N(1)	2.011	Cl	-0.85
Zn-N(2)	2.036	N(1)	-0.71
Zn-S(2)	2.260	N(2)	-0.70
Pt-S(1)	2.285	S(1)	-0.28
		S(2)	-0.66
		Pt	0.58

Complex X			
Bond lengths (Å)		NBO charges (e)	
Zn-Cl	2.389	Zn	1.54
Zn-N(1)	2.047	Cl	-0.84
Zn-S(2)	2.333	N(1)	-0.68
Zn-S(3)	2.272	S(1)	-0.29
Pt-S(1)	2.295	S(2)	-0.70
		S(3)	-0.67
		Pt	0.59

Complex XI			
Bond lengths (Å)		NBO charges (e)	
Zn-Cl	2.277	Zn	1.59
Zn-N(1)	2.101	Cl	-0.84
Zn-N(2)	2.092	N(1)	-0.68
Zn-S(1)	2.498	N(2)	-0.68
Zn-S(2)	2.552	S(1)	-0.24
Pt-S(1)	2.287	S(2)	-0.32
Pt-S(2)	2.296	Pt	0.44

Complex XII			
Bond lengths (Å)		NBO charges (e)	
Zn-Cl	2.365	Zn	1.54
Zn-N(1)	2.056	Cl	-0.83
Zn-S(2)	2.372	N(1)	-0.69
Zn-S(3)	2.245	S(1)	-0.26
Pt-S(1)	2.303	S(2)	-0.34
Pt-S(2)	2.284	S(3)	-0.66
		Pt	0.42

Fig. 6. Resultant optimized structures of initial monothiolate and dithiolate bridged Zn-Pt binuclear pentacoordinate Zn complexes of Cys_2His_2 and Cys_3His ZF cores with Cl^- as the fifth ligand to Zn. The M-L bond distances and NBO charges on the metals and the ligating atoms are also tabulated.

diffuseness of the sulphide ion to an extent that in the dithiolate bridged Cys_3His complex (**VIII**) the ∠S-Zn-S measures as small as 83°, which is a huge reduction compared to the average 115° measured in the core by itself. Thus it can be inferred that effective van der Waals radius of sulphide ligands depend on the nature of stabilizing interactions around them. Additionally, the lack of directionality in Zn-L bonds is once again visible in these complexes. Thus the geometry of the complex is not merely dependent on the metal and its ligands but also the secondary coordination sphere interactions. Hence in ZF cores, a strongly stabilizing interaction such as Lys-thiolate, may just not only contribute towards the thermodynamic stability of the core but may dictate its geometry.

Therefore it seems that providing enough stabilizing interaction to reduce the charge repulsion between the anionic ligands may be the key towards modelling coordination sphere expansion in ZF cores. In these structures the amide moieties do not serve the purpose of stabilization since better stabilization is provided by the Pt or amine groups. Hence they will be used in the models below only when required. Further, because the geometry around Pt varies little in most of the calculations and the bonding around Zn is the focus of this paper, we will discuss only the geometry and bonding around Zn hereafter.

Modelling Coordination Sphere Expansion of ZF cores

In order to test the possibility of Zn undergoing coordination sphere expansion, we constructed models by adding Cl^- as the fifth ligand to Zn in each of the above complexes **V-VIII**, as

Metallomics Accepted Manuscript

implicated by our previous studies.[22,25] At first, models with the initial geometries in square pyramidal conformation, with chloride at the apex and all other ligands at the base, were constructed. In the case of Cys_2His_2 models, the thiolates were modelled simply as thiomethane while for Cys_3His models, two of the thiolates were modelled as thiomethane and the other one as 3-sulfanylpropanamide. Geometry optimization of these models in gas phase predicted only the dithiolate bridged Cys_2His_2 complex, **XI** (Fig. 6), to be a minimum with zinc in the desired pentacoordinate conformation. Here, Zn^{2+} is slightly out of the plane formed by the imidazoles and thiolates as can be seen from the average ∠Cl-Zn-L of 103.1 ± 3.4°. The ∠S-Zn-S measures 77.2°, the average ∠S-Zn-N is 89.8 ± 0.6° and ∠N-Zn-N is 91.8°. The M-L bond lengths and NBO charges on the metals and ligating atoms are listed in Fig. 6. The Zn-Cl bond length is close to the average experimental value (Table S6) and the Zn-N bond length is slightly longer than those observed in the original Cys_2His_2 core (**III**) and the tetracoordinate dithiolate bridged analogue (**VIII**) discussed above. The Zn-S bond lengths are at the upper limit of those observed in protein crystal structures.[34] The slightly longer Zn-S(2) bond length is due to steric repulsion between the methyl group of the thiolate and the Cl^- ligand. Compared to its tetracoordinate analogue, the charge on zinc did not change upon addition of the Cl^- ligand, which indicates little charge transfer between them. Additionally, being monovalent, Cl^- retains most of its charge density. The charge on both the S atoms is effectively reduced due to covalent bonding with Pt. Now, Cl^- being the only larger ion with higher charge density, it seems that the repulsion between the ligands have been minimized enough through these stabilizing interactions. Thus the complex may exist in this conformation under favourable conditions.

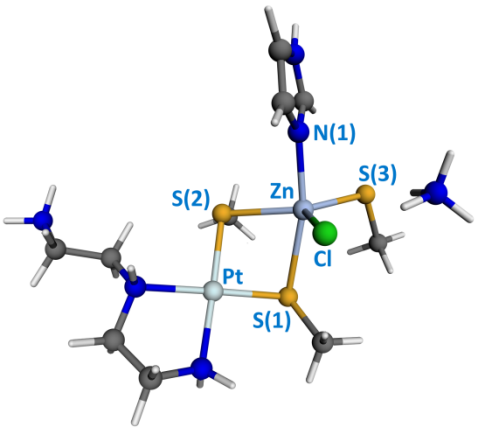

{NH_4[ZnCl(Cys)(His)(μ-Cys)$_2$Pt(dien)]}$^+$ (XIII)

Bond lengths (Å)		NBO charges (e)	
Zn-Cl	2.425	Zn	1.51
Zn-N(1)	2.169	Cl	-0.80
Zn-S(1)	2.669	N(1)	-0.67
Zn-S(2)	2.415	S(1)	-0.27
Zn-S(3)	2.316	S(2)	-0.31
Pt-S(1)	2.286	S(3)	-0.60
Pt-S(2)	2.294	Pt	0.45

Fig. 7. Optimized structures of dithiolate bridged Zn-Pt binuclear pentacoordinate Zn complexes of Cys_3His ZF cores. The M-L bond distances and NBO charges on the metals and the ligating atoms are also tabulated.

During the optimization, the structures of the initially monothiolate bridged complexes of Cys_2His_2 and Cys_3His ZF cores dissociated to form association complexes, **IX** and **X** (Fig. 6). Each of these comprised a square planar [Pt(dien)(Cys)] and a tetrahedral [ZnCl(Cys)$(His)_2$] or [ZnCl$(Cys)_2$(His)] moiety. The complexes are held together by hydrogen bonding and van der Waals interactions. As far as structure of the initially dithiolate bridged pentacoordinate Cys_3His complex, one of the bridging thiolates dissociated from Zn completely leading to a monothiolate bridged complex, **XII** (Fig. 6). In these three latter complexes, the Zn-Cl bonds are a bit longer than in those observed experimentally (Table S6). The Zn-S bond lengths fall within normal range and a little longer for the Cys_3His core due to the higher charge on the cluster. The Cl and S(2) are involved in hydrogen bonding with the amine from the dien and this explains the observed elongation in their bond lengths to Zn. The ∠L-Zn-L of S and Cl are governed by stabilizing hydrogen bonding interactions and coulomb repulsions while for N, it is majorly dictated by van der Waals attraction between $C_{\delta2/\varepsilon1}$-H of imidazole and S, Cl or backbone amide. The instability of these complexes is obviously due to charge repulsion from Cl^- and non-bridging thiolates. In order to minimize these repulsions we tried modelling trigonal bipyramidal conformations of these unstable species, where we placed the Cl^- and non-bridging thiolates in the trigonal plane in order to minimize the repulsions. We also tried protonating the non-bridging thiolates hoping to reduce the charge repulsion. But these attempts were not fruitful. Finally we considered to introduce more charge stabilization by including ammonium ions, which would mimic the stabilizing effect from Lys groups which are prevalent around the Zn core of ZF proteins. Now, we were able to locate a minimum energy conformer of the dithiolate bridged Cys_3His core with zinc in trigonal bipyramidal geometry, **XIII** (Fig. 7).

The structure of **XIII** has the imidazole and one of the bridging thiolates in the axial positions and the other three ligands forming the trigonal plane. An ammonium molecule interacts with the Cl^- and the non-bridging thiolate. The average ∠N-Zn-L (L = ligands in trigonal plane) is 90.7 ± 1.1°, which is perfect for the geometry. However, the angle between S(1), the other axial ligating atom, and the planar ligands varies a lot due to an elongated Zn-S(1) bond; the ∠S(1)-Zn-S(2) is 75.1°, ∠S(1)-Zn-S(3) is 100.1° and ∠S(1)-Zn-Cl is 92.3°. The ∠S(2)-Zn-S(3) being 133.6° is the largest and is so due to steric repulsion from the methyl group on S(2) rather than charge repulsion between the S atoms. The ∠Cl-Zn-S(3) is 114.3° and ∠Cl-Zn-S(2) is 112.0°. The ∠Cl-Zn-S(3) is dictated by the stabilizing hydrogen bonding interaction from the ammonium ion. Two of the hydrogens from the ammonium ion are involved in hydrogen bonding (2.0 Å) with Cl and S(2) each. The Zn-Cl and Zn-N bond distances are longer than in any of the other structures reported here. The closest geometry for comparison of imidazole environment is in the native Cys_3His model (**IV**), where the thiolates are in a near planar conformation due to repulsion among themselves, which leads to elongation of the Zn-N bond length. Thus it can be assumed that the elongation in bond lengths seen here is due to repulsive interactions between the ligands. The Zn-S(2) bond length is too long but such bond lengths are observed in protein crystal structures, although not common.[34] The geometry of the

Metallomics Accepted Manuscript

trigonal planar ligands and the orientation of S(2) towards Zn suggests that a favourable interaction exists between them. An overall positive charge on the complex may be essential to stabilize the negative core, which is accomplished here by the addition of NH_4^+.

Nature of the Pentacoordinate Species

These gas phase geometry optimizations support the possibility of ZF cores undergoing coordination sphere expansion under stabilizing conditions. The vibrational frequency analyses of all the structures reported above prove that these correspond to minima on the potential energy surface. However as suggested in an appeal by Hoffmann *et al*.,[58] these species could be described as 'fleeting'. Energy comparison between the tetracoordinate and pentacoordinate states was possible in the case of Cys_2His_2 and the tetracoordinate species is roughly 9 kcal mol^{-1} more stable.

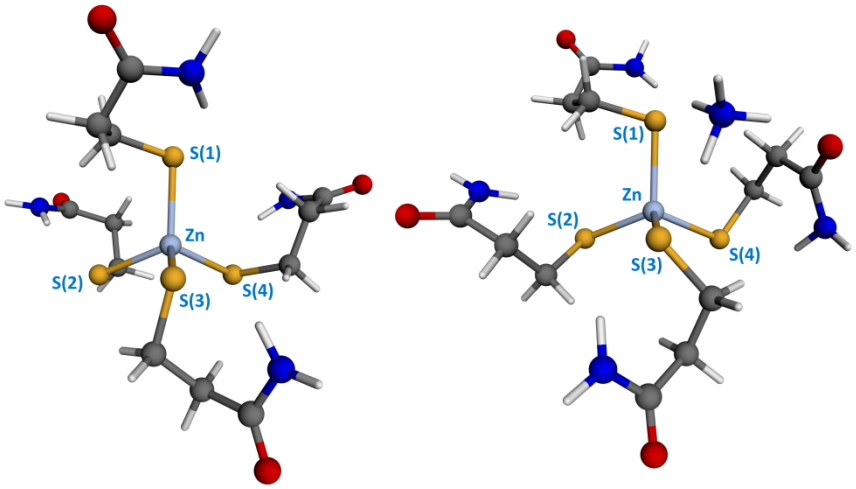

$[Zn(Cys)_4]^{2-}$ (XIV) $\{NH_4[ZnCys_4]\}^-$ (XV)

Complex XIV			
Bond lengths (Å)		NBO charges (e)	
Zn-S(1)	2.357	Zn	1.47
Zn-S(2)	2.368	S(1)	-0.67
Zn-S(3)	2.361	S(2)	-0.66
Zn-S(4)	2.367	S(3)	-0.67
		S(4)	-0.67

Complex XV			
Bond lengths (Å)		NBO charges (e)	
Zn-S(1)	2.410	Zn	1.46
Zn-S(2)	2.308	S(1)	-0.68
Zn-S(3)	2.431	S(2)	-0.66
Zn-S(4)	2.352	S(3)	-0.64
		S(4)	-0.64

Fig. 8. Optimized structures of Cys_4 ZF models: $[Zn(Cys)_4]^{2-}$ and the same in association with an ammonium ion, modelled to mimic salt bridge interaction of Lys residue. The M-L bond distances and NBO charges on the metals and the ligating atoms are also tabulated.

Thus clearly the pentacoordinate state is a local minimum on the potential energy surface. Further, low vibrational frequencies, around 75 cm^{-1}, that correspond to bond stretch of Zn-S bonds were observed, suggesting thermal instability. The effect of solvation would be an important factor that would govern the lifetime of these species. Our attempts to include solvent effect during optimization of these models were mostly unsuccessful due to convergence issues arising due to the rather shallow potential energy surface. However, the optimization of dithiolate bridged pentacoordinate Cys_2His_2 (**XI**), with solvent effect included by using the IEFPCM model and water as solvent was successful. In this structure, overall the Zn-S and Zn-N bonds were shorter by 0.02 Å while Zn-Cl bond elongated by 0.12 Å, compared to gas phase structure, which indicates stabilization in solution. The two pentacoordinate Zn cores, the structures of which are predicted to be feasible, are both dithiolate bridged and hold a net positive charge. Although the monothiolate species are predicted to be unstable, they may exist briefly as intermediates towards the dithiolate ones, as shown in one of our studies.[25] It is noteworthy that the net positive charge on these species, which may be required for their 'stability', is favoured during ESI-MS experiments in which these species were detected. Further, the C-terminal NCp7 ZF, used as a model in these studies, by itself carries a single positive charge in its holoform at neutral pH (with cysteines taken as thiolates). Thus the experimental conditions and the model system under study were both conducive to coordination sphere expansion at the Zn core.

The Effect of Salt Bridges on the Structure of ZF core

Evidently, salt bridges formed by Lys or Arg with zinc bound thiolates could be a major contributor to the structural features of ZF cores. In order to access the structural consequences of a salt bridge, we modelled such an interaction in a Cys_4 ZF core. The salt bridge was modelled using an ammonium ion in association with the sulfhydryl group, to mimic the interaction with a Lys residue. The optimized structures of the Cys_4 ZF cores by itself, $[Zn(Cys)_4]^{2-}$ (**XIV**), and the one in association with an ammonium ion, $\{NH_4[Zn(Cys)_4]^-\}$ (**XV**), along with M-L bond lengths and NBO charges of Zn and S atoms are shown in Fig. 8. The average ∠S-Zn-S is 109.5 ± 2.0°. The asymmetry in this core, seen from the standard deviation, is due to steric hindrance, since simpler models with just thiomethane yield highly symmetrical geometry (data not shown). The Zn-S bonds are longer compared to the other two ZF cores while the charge on Zn and S are comparable. Perturbation of this system by adding an ammonium ion yielded a structure, **XV**, in which the ammonium is in association with two of the sulphur atoms, S(1) and S(3). Due to this interaction, the ∠S(1)-Zn-S(3) is compressed to 105.4°, while ∠S(2)-Zn-S(4) relaxes to 113.5°. The average of the other ∠S-Zn-S is 109.4 ± 0.8°, which is closer to the ideal tetrahedral angle. The Zn-S bond for the S in association with NH_4^+ is elongated while the other Zn-S are shorter, compared to the original core. There is little charge difference on Zn and S compared to the original core, implying highly ionic interactions. Thus it is proven that salt bridge type interactions, in addition to stabilizing the unstable ZF core, significantly influence the structure of such cores.

Significance and Implications

Choice of DFT Method for Structural Zinc Models

Metallomics Accepted Manuscript

Our evaluation of DFT methods for Zn molecular systems (see supporting information) clearly indicated the importance of properly accounting for electron correlation, as indicated previously.[59] The PW91 and PBE correlation functionals performed better compared to the LYP functional. Thus the most commonly used B3LYP functional may not be the best choice for Zn molecular systems. At least for the systems investigated in this paper, due to their fragile nature, B3LYP was a poor choice as it produced longer Zn-L bond lengths leading to fragmentation easily. Another common DFT method for Zn systems found in the literature is the LSDA functional, SVWN. Our tests (not reported) showed that this functional reproduces experimental parameters remarkably well. However, use of it for (Zn, Pt) binuclear complexes revealed a tendency to overestimate Zn-Pt interaction which often resulted in distances close to bonding between the metals, which obviously is an artefact. Additionally

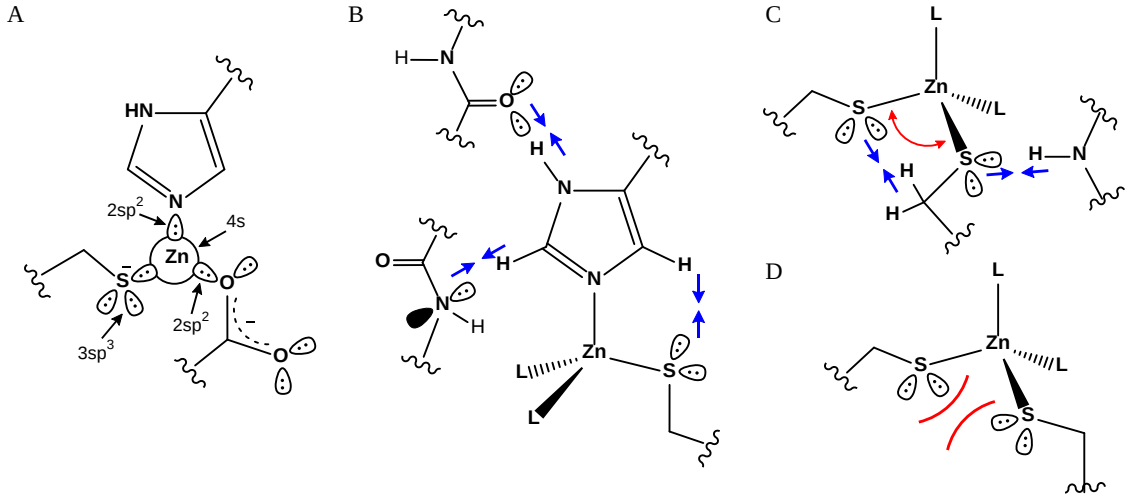

Fig. 9. Factors affecting coordination geometry of zinc in protein environment. The hybridization schemes shown in A are derived from natural electron configuration obtained through NPA (Table S1).

LSDA is known to overbind and therefore is not advisable for energy calculations.[60] Variation of the exchange functional produced little effect. Hence from our test we recommend the use of PW91 or PBE correlations functionals which have been shown to reproduce both geometric and energy values to a reasonable accuracy.[61-63] Further, the geometric parameters were highly sensitive to changes in basis functions, especially diffuse and polarization functions. However, global addition of these functions on all atoms was not the best method. Instead, the best result for structural zinc models were produced when diffuse functions were used just on anionic ligating atoms (S and Cl) and higher order polarization on all ligating atoms and Zn. Combining this with a previous result that diffuse functions are essential on O to model zinc bound carboxylate,[64] the method can be generalized and expanded to model all protein zinc sites. Although triple-ζ quality basis sets were used on all atoms for our applications, it may not be essential as even double-ζ quality basis sets gave reasonable results.

The Essentials to Unravel the Dynamics at Biological Zinc Sites

The dynamics at biological zinc sites is a topic of current focus. Several studies have used modern methods to elucidate the dynamic changes in both catalytic and structural sites. Concurrently, interesting findings in biology point towards a dynamic role of zinc, which have previously been unrecognised. In order to explore these new paradigms, experimental and computational methods are required to augment each other. For instance, transient coordination sphere expansions have been predicted by XAS, XAFS and MD studies[65-67] and confirmed by X-ray crystal strucutres.[68] In another case, QM methods have been proposed to refine medium and low resolution X-ray crystal structures.[69] However, QM methods are both computationally and temporally expensive. But due to lack of parameters for zinc sites, dynamic changes such as coordination sphere expansion needs to be addressed using QM methods. Therefore simpler force field models are being constantly developed to parameterize zinc environment in proteins. As our understanding about the nature of bonding of zinc and its ligands improves, better force fields can be created. For example, recent improvements of including charge transfer and polarization effects have been promising.[70,71]

The following finding from this study about the nature of bonding in zinc would be helpful for modelling zinc environment in proteins (Fig. 9): Firstly, Zn-L bonds are majorly ionic and in addition, the covalent character is contributed by its 4s orbital. This signifies that the geometry and the coordination number on zinc would be dictated by the ligands and protein environment. Further, this clearly accounts for lack directionality and flexibility of bonding in zinc. Since the 3d orbital in Zn^{2+} is completely filled, it does not contribute towards bonding and the 4p orbital is too high in energy compared to the occupied orbitals of the ligands for any appreciable overlap. This trend is supported by an X-ray emission spectroscopy study of zinc sulphide.[72] Hence textbook based concepts such as 18 electron rule or 3d4s and 4s4p hybridization, which can be found in the literature today needs to be reconsidered.[42,73,74] Secondly, the ligand geometries are oriented in such a way to maximize coulomb attraction. Since the common biological ligands are multivalent and may be simply considered to feature hybridized orbitals, an orientation where their lone pairs are directed towards zinc would result in the best coulomb attraction and therefore favoured. This is a factor that affects the binding preference of zinc, as seen in the case of the recently predicted inhibitory binding sites in caspase-

Metallomics Accepted Manuscript

3.[9] In this case, Zn^{2+} was shown to preferentially bind to a histidine and a methionine rather than to the histidine and a cysteine, due to lack of flexibility in the cysteine residue. Therefore, directionality of ligands should be accounted for in order to get reasonable results. Thirdly, as evident from these calculations, since zinc can accepts just around 0.5 electrons, coulomb repulsion becomes increasingly dominant with the number of negatively charged ligands. Thus it is equally important to define the charges on the ligating atoms precisely as it is for zinc. It should be noted that because our model systems are larger and mimics protein environment better than those previously reported, the variation in charge density on zinc and ligands is lesser. Hence results from minimal models should be treated with care. Fourthly, the geometry of the primary coordination sphere can be altered by steric and stabilizing electrostatic interactions in the secondary coordination sphere to a large extent. Hence it is important to account for these factors in order to properly describe geometry of the zinc site at a given time.

Pharmacological and Biological Implications

The predicted pentacoordinate species are evidently made possible by charge reduction on thiolates as a result of coordination to Pt. This presents a strategy to facilitate zinc chelation from protected ZF cores[37] by increasing their susceptibility to accept another ligand. Further, characterization of these adducts is significant in a pharmacological sense because it helps understand the modes of interaction of Pt drugs with proteins and DNA. Given the possibility of coordination sphere expansion of zinc in these adducts, dynamic conversion of structural zinc into a transient catalytic centre may be a mechanism for nucleic acid cleavage. Although no such specific conversion has been reported, the hydrolytic activity of a mutant ZF with one Cys and three His is known.[75]

In addition to the primary covalent interaction between the zinc bound thiolates and Pt, the amines of the dien ligand stabilize the non-bridged thiolates and chloride ligands. Although these are electrostatic in nature, there is directionality arising due to the lone pairs on these ligands as discussed above. Given the flexible nature of zinc itself, these interactions are found to define the geometry of the ligands involved, which is apparent from the bond angles. This raises an important question whether such stabilizing interactions, even if transient would affect the geometry of zinc sites. Secondary coordination sphere interactions are known to be important to stabilize ZF cores and in assisting catalysis. However, their contribution to dynamics remains to be explored. Our calculations suggest that stronger interactions such as from lysine or arginine may significantly influence the geometry at zinc sites. Hence ZF cores may be more dynamic than conceived so far.

Conclusions

Here, by using appropriate ZF models and an accurate DFT method, we have shown that the factors influencing the geometry and the dynamics at zinc finger sites are the directionality of the ligand, electronic charges on zinc and the ligating atoms, steric and stabilizing interactions from the secondary coordination sphere. Bonding between zinc and its ligands is prominently ionic with a smaller covalent contribution involving the 4s orbital of zinc. Across the various ZF cores, the observed larger ∠S-Zn-L and elongation of Zn-L distance with increasing number of thiolate ligands can be correlated to the greater Coulomb repulsion arising from the diffuse anionic sulphur atoms. Interaction of $[Pt(dien)]^{2+}$ with the zinc bound sulphur atoms effectively reduces the charge density on them, allowing smaller bond angles and hence room for an extra ligand. However, as inferred from the predicted instability of monothiolate bridged pentacoordinate complexes, all of the thiolates need to be sufficiently stabilized in order for coordination sphere expansion. Thus, as predicted, the dithiolate bridged pentacoordinate complexes may exist. The arrangement of the diffuse anionic ligands around zinc in a fashion to minimize repulsion is critical. Further, the overall charge of the molecule and other stabilizing secondary coordination sphere interactions may play a role in stabilizing the pentacoordinate species. Through this study a comprehensive model to explain and predict bonding in zinc complexes has been developed.

Acknowledgments

This work was supported by NSF-CHE-1058726.

Notes and references

[a] *Department of Chemistry, Virginia Commonwealth University, Richmond, VA 23284-2006, USA. Fax: 804-828-8599; Tel: 804-828-6320; E-mail: npfarrell@vcu.edu*

† Electronic Supplementary Information (ESI) available: [details of any supplementary information available should be included here]. See DOI: 10.1039/b000000x/

1 S. F. Sousa, A. B. Lopes, P. A. Fernandes and M. J. Ramos, *Dalton Trans.*, 2009, **38**, 7946-7956.
2 D. S. Auld, *Biometals*, 2001, **14**, 271-313.
3 K. A. McCall, C. Huang and C. A. Fierke, *J. Nutr.*, 2000, **130**, 1437S-1446S.
4 Y. Lin, V. Dotsch, T. Wintner, K. Peariso, L. C. Myers, J. E. Penner-Hahn, G. L. Verdine and G. Wagner, *Biochemistry*, 2001, **40**, 4261-4271.
5 J. Penner-Hahn, *Curr. Opin. Chem. Biol*., 2007, **11**, 166-171.
6 E. Bombarda, H. Cherradi, N. Morellet, B. P. Roques and Y. Mely, *Biochemistry*, 2002, **41**, 4312-4320.
7 U. Heinz, M. Kiefer, A. Tholey and H. W. Adolph, *J. Biol. Chem.*, 2005, **280**, 3197-3207.
8 W. Maret, *Biometals*, 2013, **26**, 197-204.
9 A. G. Daniel, E. J. Peterson and N. P. Farrell, *Angew. Chem. Int. Ed*., 2014, **53**, 4098-4101.
10 S. Iuchi and N. Kuldell, *Zinc Finger Proteins: From Atomic Contact to Cellular Function.*, Kluwer Academic, New York, 2005.
11 O. Seneque and J. Latour, *J. Am. Chem. Soc.*, 2010, **132**, 17760-17774.
12 L. M. Green and J. M. Berg, *Proc. Natl. Acad. Sci. U. S. A.*, 1990, **87**, 6403-6407.
13 A. J. Bird, S. Swierczek, W. Qiao, D. J. Eide and D. R. Winge, *J. Biol. Chem.*, 2006, **281**, 25326-25335.
14 Y. Lee, Y. Wang, Y. Duh, H. S. Yuan and C. Lim, *J. Am. Chem. Soc.*, 2013, **135**, 14028-14031.
15 W. Maret and Y. Li, *Chem. Rev.*, 2009, **109**, 4682-4707.
16 G. M. Clore, J. G. Omichinski and A. M. Gronenborn, *J. Am. Chem. Soc.*, 1991, **113**, 4350-4351.
17 W. Maret, *Biometals*, 2009, **22**, 149-157.
18 G. Wellenreuther, M. Cianci, R. Tucoulou, W. Meyer-Klaucke and H. Haase, *Biochem. Biophys. Res. Commun.*, 2009, **380**, 198-203.
19 A. I. Anzellotti and N. P. Farrell, *Chem. Soc. Rev.*, 2008, **37**, 1629-1651.

Metallomics Accepted Manuscript

20 R. A. Musah, *Curr. Top. Med. Chem.*, 2004, **4**, 1605-1622.
21 H. de Rocquigny, V. Shvadchak, S. Avilov, C. Z. Dong, U. Dietrich, J. L. Darlix and Y. Mely, *Mini Rev. Med. Chem.*, 2008, **8**, 24-35.
22 Q. A. de Paula, J. B. Mangrum and N. P. Farrell, *J. Inorg. Biochem.*, 2009, **103**, 1347-1354.
23 A. I. Anzellotti, Q. Liu, M. J. Bloemink, J. N. Scarsdale and N. Farrell, *Chem. Biol.*, 2006, **13**, 539-548.
24 S. D. Tsotsoros, A. B. Bate, M. G. Dows, S. R. Spell, C. A. Bayse and N. P. Farrell, *J. Inorg. Biochem.*, 2014, **132**, 2-5.
25 E. Almaraz, Q. A. de Paula, Q. Liu, J. H. Reibenspies, M. Y. Darensbourg and N. P. Farrell, *J. Am. Chem. Soc.*, 2008, **130**, 6272-6280.
26 H. Vahrenkamp, *Dalton Trans.*, 2007, , 4751-4759.
27 W. Maret, *Methods Enzymol.*, 2002, **348**, 230-237.
28 A. F. Parisi and B. L. Vallee, *Am. J. Clin. Nutr.*, 1969, **22**, 1222-1239.
29 S. Yamasaki, K. Sakata-Sogawa, A. Hasegawa, T. Suzuki, K. Kabu, E. Sato, T. Kurosaki, S. Yamashita, M. Tokunaga, K. Nishida and T. Hirano, *J. Cell Biol.*, 2007, **177**, 637-645.
30 H. Haase and L. Rink, *Metallomics*, 2014, **6**, 1175-1180.
31 K. D. Kroncke and L. O. Klotz, *Antioxid. Redox Signal.*, 2009, **11**, 1015-1027.
32 C. A. Blindauer, *J. Inorg. Biochem.*, 2013, **121**, 145-155.
33 N. Dimakis, M. J. Farooqi, E. S. Garza and G. Bunker, *J. Chem. Phys.*, 2008, **128**, 115104.
34 M. B. Peters, Y. Yang, B. Wang, L. Fusti-Molnar, M. N. Weaver and K. M. Merz Jr, *J. Chem. Theory Comput.*, 2010, **6**, 2935-2947.
35 J. R. Calhoun, W. Liu, K. Spiegel, M. Dal Peraro, M. L. Klein, K. G. Valentine, A. J. Wand and W. F. DeGrado, *Structure*, 2008, **16**, 210-215.
36 C. J. Cramer and D. G. Truhlar, *Phys. Chem. Chem. Phys.*, 2009, **11**, 10757.
37 Y. M. Lee and C. Lim, *J. Mol. Biol.*, 2008, **379**, 545-553.
38 T. Dudev and C. Lim, *J. Am. Chem. Soc.*, 2000, **122**, 11146-11153.
39 T. Dudev and C. Lim, *J. Am. Chem. Soc.*, 2007, **129**, 12497-12504.
40 A. T. Maynard, M. Huang, W. G. Rice and D. G. Covell, *Proc. Natl. Acad. Sci. U. S. A.*, 1998, **95**, 11578-11583.
41 Y. Lee and C. Lim, *J. Am. Chem. Soc.*, 2011, **133**, 8691-8703.
42 Y. Lee, Y. Lin and C. Lim, *J. Chin. Chem. Soc.*, 2014; 2013, **61**, 142-150.
43 D. Picot, G. Ohanessian and G. Frison, *Inorg. Chem.*, 2008, **47**, 8167-8178.
44 T. Simonson and N. Calimet, *Proteins*, 2002, **49**, 37-48.
45 T. Dudev and C. Lim, *J. Am. Chem. Soc.*, 2002, **124**, 6759-6766.
46 Y. Lin and C. Lim, *J. Am. Chem. Soc.*, 2004, **126**, 2602-2612.
47 D. Picot, G. Ohanessian and G. Frison, *Chem. Asian J.*, 2010, **5**, 1445-1454.
48 T. Dudev and C. Lim, *J. Chin. Chem. Soc.*, 2003, **50**, 1093-1102.
49 A. T. Maynard and D. G. Covell, *J. Am. Chem. Soc.*, 2001, **123**, 1047-1058.
50 A. D. Becke, *J. Chem. Phys.*, 1993, **98**, 5648.
51 C. Lee, W. Yang and R. G. Parr, *Phys. Rev. B*, 1988, **37**, 785-789.
52 J. Slater, *The Self-Consistent Field for Molecular and Solids, Quantum Theory of Molecular and Solids*, Vol. 4, McGraw-Hill, New York, , 1974.
53 S. H. Vosko, L. Wilk and M. Nusair, *Can. J. Phys.*, 1980, **58**, 1200-1211.
54 A. J. H. Wachters, *J. Chem. Phys.*, 2003, **52**, 1033-1036.
55 P. J. Hay, *J. Chem. Phys.*, 2008, **66**, 4377-4384.
56 M. J. Frisch, G. W. Trucks, H. B. Schlegel, G. E. Scuseria, M. A. Robb, J. R. Cheeseman, J. Montgomery J. A., T. Vreven, K. N. Kudin, J. C. Burant, J. M. Millam, S. S. Iyengar, J. Tomasi, V. Barone, B. Mennucci, M. Cossi, G. Scalmani, N. Rega, G. A. Petersson, H. Nakatsuji, M. Hada, M. Ehara, K. Toyota, R. Fukuda, J. Hasegawa, M. Ishida, T. Nakajima, Y. Honda, O. Kitao, H. Nakai, M. Klene, X. Li, J. E. Knox, H. P. Hratchian, J. B. Cross, V. Bakken, C. Adamo, J. Jaramillo, R. Gomperts, R. E. Stratmann, O. Yazyev, A. J. Austin, R. Cammi, C. Pomelli, J. W. Ochterski, P. Y. Ayala, K. Morokuma, G. A. Voth, P. Salvador, J. J. Dannenberg, V. G. Zakrzewski, S. Dapprich, A. D. Daniels, M. C. Strain, O. Farkas, D. K. Malick, A. D. Rabuck, K. Raghavachari, J. B. Foresman, J. V. Ortiz, Q. Cui, A. G. Baboul, S. Clifford, J. Cioslowski, B. B. Stefanov, G. Liu, A. Liashenko, P. Piskorz, I. Komaromi, R. L. Martin, D. J. Fox, T. Keith, M. A. Al-Laham, C. Y. Peng, A. Nanayakkara, M. Challacombe, P. M. W. Gill, B. Johnson, W. Chen, M. W. Wong, C. Gonzalez and J. A. and Pople, *Gaussian 03, Revision D.02*, Gaussian, Inc., Wallingford CT, 2004.
57 I. L. Alberts, K. Nadassy and S. J. Wodak, *Protein Sci.*, 1998, **7**, 1700-1716.
58 R. Hoffmann, P. v. R. Schleyer and H. F. Schaefer, *Angew. Chem. Int. Ed.*, 2008, **47**, 7164-7167.
59 U. Ryde, *Eur. Biophys. J.*, 1996, **24**, 213-221.
60 W. Kohn, A. D. Becke and R. G. Parr, *J. Phys. Chem.*, 1996, **100**, 12974-12980.
61 M. N. Weaver, K. M. Merz Jr, D. Ma, H. J. Kim and L. Gagliardi, *J. Chem. Theory Comput.*, 2013, **9**, 5277-5285.
62 S. Paranthaman, K. Hong, J. Kim, D. E. Kim and T. K. Kim, *J. Phys. Chem. A*, 2013, **117**, 9293-9303.
63. E. A. Amin, D. G. Truhlar, *J. Chem. Theory Comput.* **2008**, *4*, 75-85.
64 U. Ryde, *Biophys. J.*, 1999, **77**, 2777-2787.
65 O. Kleifeld, A. Frenkel, J. M. Martin and I. Sagi, *Nat. Struct. Mol. Biol.*, 2003, **10**, 98-103.
66 J. Koca, C. Zhan, R. C. Rittenhouse and R. L. Ornstein, *J. Comput. Chem.*, 2003, **24**, 368-378.
67 P. Giannozzi, K. Jansen, G. La Penna, V. Minicozzi, S. Morante, G.C. Rossi, F. Stellato *Metallomics*, 2012, **4**, 156-165.
68 P. J. Baker, K. L. Britton, M. Fisher, J. Esclapez, C. Pire, M. J. Bonete, J. Ferrer and D. W. Rice, *Proc. Natl. Acad. Sci. U. S. A.*, 2009, **106**, 779-784.
69 X. Li, S. A. Hayik and K. M. Merz Jr, *J. Inorg. Biochem.*, 2010, **104**, 512-522.
70 D. V. Sakharov and C. Lim, *J. Am. Chem. Soc.*, 2005, **127**, 4921-4929.
71 T. Zhu, X. Xiao, C. Ji and J. Z. Zhang, *J. Chem. Theory Comput.*, 2013, **9**, 1788-1798.
72 R. A. Mori, E. Paris, G. Giuli, S. G. Eeckhout, M. Kavcic, M. Zitnik, K. Bucar, L. G. Pettersson, P. Glatzel, *Inorg. Chem.* **2010**, *49*, 6468-6473.
73 M. Laitaoja, J. Valjakka and J. Jänis, *Inorg. Chem.*, 2013, **52**, 10983-10991.
74 Y. P. Pang, *Proteins*, 2001, **45**, 183-189.
75 S. Negi, M. Itazu, M. Imanishi, A. Nomura, Y. Sugiura, *Biochem. Biophys. Res. Commun.*, 2004, **325**, 421-425.

Metallomics Accepted Manuscript